

Published in final edited form as:

Astron Astrophys. 2016 March ; 587: . doi:10.1051/0004-6361/201527531.

A rigorous detection of interstellar CH₃NCO: An important missing species in astrochemical networks^{*,**}

J. Cernicharo¹, Z. Kisiel², B. Tercero¹, L. Kolesníková³, I.R. Medvedev^{4,5}, A. López¹, S. Fortman⁴, M. Winnewisser⁴, F. C. de Lucia⁴, J. L. Alonso³, and J.-C. Guillemin⁶

¹Grupo de Astrofísica Molecular. Instituto de CC. de Materiales de Madrid (ICMM-CSIC). Sor Juana Inés de la Cruz 3, Cantoblanco, 28049 Madrid, Spain ²Laboratory of Mm- and Submm-Spectroscopy. Institute of Physics, Polish Academy of Sciences. Al. Lotnikow 32/46, 02-668 Warszawa, Poland ³Grupo de Espectroscopía Molecular (GEM), Edificio Quifima, Área de Química-Física, Laboratorios de Espectroscopía y Bioespectroscopía, Parque Científico UVA, Unidad Asociada CSIC, Universidad de Valladolid, 47011 Valladolid, Spain ⁴Department of Physics, The Ohio State University, 191 W. Woodruff Ave, Columbus, OH 43210, USA ⁵Wright State University, 3640 Colonel Glenn Hwy, Dayton, OH 45435, USA ⁶Institut des Sciences Chimiques de Rennes, Ecole Nationale Supérieure de Chimie de Rennes, CNRS, UMR 6226, 11 Allée de Beaulieu, CS 50837, 35708 Rennes Cedex 7, France

Abstract

The recent analysis of the composition of the frozen surface of comet 67P/Churyumov-Gerasimenko has revealed a significant number of complex organic molecules. Methyl isocyanate (CH₃NCO) is one of the more abundant species detected on the comet surface. In this work we report extensive characterization of its rotational spectrum resulting in a list of 1269 confidently assigned laboratory lines and its detection in space towards the Orion clouds where 399 lines of the molecule have been unambiguously identified. We find that the limited mm-wave laboratory data reported prior to our work require some revision. The abundance of CH₃NCO in Orion is only a factor of ten below those of HNC and CH₃CN. Unlike the molecular abundances in the coma of comets, which correlate with those of warm molecular clouds, molecular abundances in the gas phase in Orion are only weakly correlated with those measured on the comet surface. We also compare our abundances with those derived recently for this molecule towards Sgr B2 (Halfen et al. 2015). A more accurate abundance of CH₃NCO is provided for this cloud based on our extensive laboratory work.

jose.cernicharo@csic.es (JC) & kisiel@ifpan.edu.pl (ZK).

*This paper makes use of the following ALMA data: ADS/JAO.ALMA#2011.0.00009.SV. ALMA is a partnership of ESO (representing its member states), NSF (USA), and NINS (Japan) with NRC (Canada), NSC, and ASIAA (Taiwan), and KASI (Republic of Korea), in cooperation with the Republic of Chile. The Joint ALMA Observatory is operated by ESO, AUI/NRAO, and NAOJ. This work was also based on observations carried out with the IRAM 30-meter telescope. IRAM is supported by INSU/CNRS (France), MPG (Germany), and IGN (Spain).

**Table A.6 is available at CDS.

Keywords

ISM: abundances; ISM: clouds; ISM: individual objects (Orion KL); ISM: molecules; Methods: laboratory: molecular; Molecular data

1 Introduction

Ice mantles on dust grains are formed from the accretion of gas phase molecules during the gravitational collapse of clouds that form new stars and their planetary systems. Surface reactions increase the chemical complexity of the mantles which, when their temperature rises, release their frozen molecular material to the gas phase (Herbst and van Dishoeck 2009). The gas and dust material of the cloud cores formed during the gravitational collapse participate in the formation of giant gas planets and rocky bodies such as comets, asteroids, and the Earth. Comets are considered to be a repository of information on their frozen surface of the gas and dust composition of the primitive solar nebula. As they approach the Sun in their journey their surface ices start to evaporate and to create a coma of gas and dust that has been extensively studied at all wavelengths (Bockelée-Morvan et al. 2000; Crovisier 2006; Mumma and Charnley 2011). A good correlation has been found between the type of molecules detected in the coma of comets and those of warm molecular clouds (Bockelée-Morvan et al. 2000; Biver et al. 2015).

The Cometary Sampling and Composition (COSAC) experiment aboard Rosetta's Philae lander has measured in situ abundances of the main components of the surface of comet 67P/Churyumov-Gerasimenko (Goesmann et al. 2015). Most of the "gas on the rocks" species assigned by COSAC are well-known interstellar molecules. However, many of the species detected by COSAC have not been observed in the coma of previously observed comets (Goesmann et al. 2015), while some organic molecules observed in the coma of comets are not detected by COSAC. Nevertheless, the coma organics can be formed by UV irradiation of the ices forming alcohols and carbonyls from CO and H₂O ices (Muñoz Caro & Dartois 2013). Among the organic molecules detected on the surface of the comet, only one was not detected in space, methyl isocyanate (CH₃NCO), which could potentially contribute to the mass peak $m/z=57$ of COSAC. Although it is a molecule of potential relevance, to our knowledge it has not been included in any astrochemical network, and to date its detection has only been reported towards Sgr B2 based on a reduced number of lines (Halfen et al. 2015), whereas on 67P/Churyumov-Gerasimenko it was identified as one of the most abundant molecules after water (Goesmann et al. 2015). The most promising interstellar clouds in which to search for CH₃NCO are hot cores and hot corinos.

In 2006 we started a sensitive line survey in the millimetre domain (80–280 GHz) of Orion using the IRAM 30m radio telescope (Tercero et al. 2010) with the goal of fully characterizing its chemical composition (see Appendix B). However, owing to the high kinetic temperature of the gas, $T_K \simeq 100\text{--}300$ K, many rotational and vibrational levels of abundant species are populated, producing a forest of spectral lines. Around 15000 spectral features were initially detected of which 8000 were unassigned. A systematic work programme in spectroscopic laboratories was started, which allowed us to significantly

reduce the number of unidentified lines and to detect new molecules such as NH_3D^+ (Cernicharo et al. 2013; Domenech et al. 2013), $\text{CH}_3\text{COOCH}_3$ (Tercero et al. 2013), and $\text{CH}_3\text{OCH}_2\text{CH}_3$ (Tercero et al. 2015).

In this Letter we report on the complete laboratory spectroscopic characterization of CH_3NCO and the detection of 399 of its lines in Orion. We also discuss the spectroscopic data used by Halfen et al. (2015) and comment on their column density estimations towards Sgr B2.

2 Spectroscopy

CH_3NCO was initially searched for in our Orion data by using the available sub-40 GHz microwave spectroscopic work for this species (Koput 1986). However, irrespective of the usual problems of extrapolation outside the data region, we faced additional problems affecting the rotational spectrum of this molecule (see Fig. 1). Koput complemented his thorough experimental investigation of the 8–40 GHz region by Stark spectroscopy with analysis based on fitting a five-dimensional, quasi-symmetric top Hamiltonian. He was unable to fit the measured transition frequencies to experimental accuracy, but he reached unambiguous assignment of rotational transitions in many internal rotation substates of the ground and the two lowest excited states of the CNC bending vibrational mode (Koput 1986). The very low effective barrier to internal rotation, $V_3=21\text{ cm}^{-1}$, was found to result in a series of low-lying internal rotor states, with the distribution close to that of the free rotor pattern, and estimated energies relative to the $m=0$ ground state of 8.4 cm^{-1} for the $m=1$ substate, 36.8 cm^{-1} for $m=2$, 79.7 and 80.3 cm^{-1} for the two nearly degenerate $m=3$ substates, and 140.6 cm^{-1} for $m=4$. The next higher vibrational state was found to be the first excited state of the CNC bending mode, $v_b=1$ at 182.2 cm^{-1} . That state, in turn, carries its own stack of internal rotor states, and so on. The resulting high state density and considerable vibration-rotation coupling are the main reason why the laboratory understanding of the rotational spectrum of this molecule has been considerably delayed.

In order to derive a reliable CH_3NCO line list for astrophysical applications we decided to cut through these problems by using the procedure described in detail in Appendix A and already discussed in two progress reports (Kisiel et al. 2010, 2015). The complete experimental spectrum in the region 40–363 GHz was measured and was first broken down into over 220 correlated line sequences. The assignment reached by Koput (1986), was then transferred to the sequences extending over the entire covered frequency range. As a result, we derived a line list for the most relevant rotational transition sequences for CH_3NCO consisting almost entirely of experimental frequencies and free from any extrapolation (see Appendix A).

Our extensive spectroscopic coverage allows line-by-line comparison (see Table A.7) with the newly reported spectroscopic data in Halfen et al. (2015), where the Koput sub-40 GHz data is extended by 21 laboratory measurements in the region 60–87.5 GHz. We find good agreement between our data and the Halfen et al. (2015) data for 13 out of the 21 reported lines, and this includes the $K_a=0,1$, $m=0$ lines crucial to the Sgr B2(N) detection in their work. At the same time we note that seven lines show intriguing frequency differences of

very close to 1 MHz between these two data sets. There is also a discrepancy in assignment concerning the line at 77107.478 MHz, which according to our analysis is $K=-2$, $m=2$ and not $K=+1$, $m=1$, and its upper level is 91 K and not 44 K. This limited agreement suggests that extrapolations made in Halfen et al. (2015) may be rather uncertain. The worst case is provided by the predicted line at 102829.29 MHz searched for in Halfen et al. (2015), since it turns out that there is no line in the laboratory spectrum within ± 10 MHz. Our comprehensive study of the laboratory spectrum of CH_3NCO showed that, even with self-consistent data, multi m -state fitting of this spectrum to experimental accuracy, and thus reliable predictions, are not yet possible. We emphasize again that the line list of 1269 lines up to 362 GHz that we report in Appendix A covers the frequency region relevant to astrophysical searches by means of actual laboratory measured frequencies.

3 Results

Once the key transitions of CH_3NCO were assigned in the laboratory, we used the resulting line list to search for this species in Orion KL. Of the 521 lines of CH_3NCO expected in the frequency coverage of the IRAM 30m data (80–280 GHz), 236 are found to be unblended with other features, and 163 are partially blended but still identifiable in the combined line profiles with the contaminating lines. The remaining 122 lines are completely blended with strong features of one or more of the most abundant species, most of them above 200 GHz where the line density in Orion becomes very considerable. None of the unblended or partially blended features is missing. Figure 2 shows a selected number of lines from our line survey and from the ALMA Science Verification (SV) data of Orion (see also Fig. B.1 which shows all 399 detected lines). The ALMA data between 213.7 and 246.7 GHz mitigates line blending owing to the high spatial resolution that distinguishes between the contributions from the different hot cores of Orion. Hence, many features that are fully contaminated in the IRAM data do appear clearly in the ALMA observations. The dipole moment of CH_3NCO is high, 2.88 D (Kasten & Dreizler 1986), but its partition function at 150 K is also very high ($\approx 3.0 \times 10^4$, see Appendix A). As a result the lines appear weaker than for species with similar abundances and dipole moments. Nevertheless, the current detection of CH_3NCO in space is based on the largest data set of convincingly assigned lines for a previously unobserved molecule. Moreover, the assigned lines correspond to the strongest unidentified features we have in our data. In the 30m and ALMA SV data the lines are strikingly prominent (see Figure 2 and B.1).

In order to derive the relative abundance of CH_3NCO with respect to other organic molecules found in the comet, we used the MADEX code (Cernicharo 2012) to model all the lines that we detected with the IRAM 30m radio telescope and the ALMA interferometer. The spatial distribution of these species, as observed with the ALMA data, together with that of CH_3NCO , is shown in Figs. 3 and B.3. At first glance the spatial distribution of CH_3NCO looks similar to that of the other species with two emission peaks, A and B symmetrically placed with respect to source n . However, a detailed inspection of these figures shows significant differences in the extent of their spatial distribution and in the position of the maxima. The most similar spatial distributions are those of CH_3NCO , HNCO , NH_2CHO , and CH_3CN . The species HDO , which traces water vapour, also shows A and B cores and is used to derive relative abundances with respect to H_2O (see Appendix B).

The remaining molecules have their emission peaks at different positions and with a different spatial extent (see Appendix B). Similar discrepancies in the spatial distribution of other molecular species in Orion have been reported (see Appendix B). Spatial correlation between species with similar chemical routes could help in assessing this new detection. In Appendix B we discuss various aspects regarding the complexity of this source and, in addition, very little is known about the formation routes of CH_3NCO so the suspicion that this species could be related to HNCO or NH_2CHO is still very tentative. The main support that the maps provide for the detection is the correlation between the two CH_3NCO maps that depict the distribution of the molecule for two different internal rotation states ($m = 0$ and $m = 1$; see Figs. 3 and B.3), which shows that the lines arise cospatially removing the possibility of their origin from different species. In Appendix B we discuss the spatial distribution of the species shown in Figs. 3 and B.3.

Because of the different angular resolution of our data, two sets of models (the methods are described in Appendix B) have been run in order to fit the molecular emission of all these species. We used one model for the single-dish data, which provides a convolved view of the source structure with the angular resolution of the 30m telescope that ranges from $10''$ to $27''$, and a different model for the ALMA data, which have an angular resolution of $1''.8 \times 1''.8$ (see Appendix B). The methyl isocyanate lines are reasonably well fitted with a kinetic temperature of 150 K. The column densities obtained from the ALMA data are given in Table B.1, which also reproduces the relative abundances of the species found by COSAC. The CO abundance in the comet was poorly determined by COSAC (Goesmann et al. 2015) and we have referred all abundances to H_2O as in the COSAC results. Table B.1 shows that CH_3NCO in the Orion clouds is 400, 15, 10, and 5 times less abundant than CH_3OH , HNCO , CH_3CN , and $\text{CH}_3\text{CH}_2\text{CN}$, respectively. However, CH_3NCO is more abundant than amines, aldehydes, and acetones.

4 Discussion

We attempted to detect two isomers of CH_3NCO : CH_3CNO (acetonitrile oxide) and CH_3OCN (methyl cyanate). The energy difference of these isomers relative to the most stable one (CH_3NCO) is 8785 cm^{-1} ($25.1 \text{ kcal mol}^{-1}$) for CH_3OCN and 20090 cm^{-1} ($57.4 \text{ kcal mol}^{-1}$) for CH_3CNO (Pasinazki & Westwood 2001). CH_3CNO has been characterized in the laboratory at millimetre wavelengths (Winnewisser et al. 1982). We derive an upper limit for its column density in Orion of $6 \times 10^{13} \text{ cm}^{-2}$, i.e., a factor of ≈ 100 below that for CH_3NCO (see Table B.1). The experimental rotational spectra of methyl cyanate were recorded recently in the millimetre wave domain from 130 to 350 GHz and more than 300 internal rotation A-E doublets were successfully analysed (Kolesniková et al., in preparation). From the predicted spectrum we also derive an upper limit to its column density of $1 \times 10^{14} \text{ cm}^{-2}$. Hence, only the most stable isomer, CH_3NCO , seems to be present in Orion. Tercero et al. (2013) found a negative detection of three isomers of methyl acetate and ethyl formate in Orion KL. López et al. (2014) also found upper limits to the abundance of the isocyanide isomers of ethyl and vinyl cyanide. A large discussion of the importance of bonding energy differences in the abundances of interstellar isomers was provided by Remijan et al. (2005). López et al. (in preparation) address the detection and abundances of two isomers of methyl formate in Orion KL.

We have searched for CH₃NCO toward a cold prestellar core, B1-b, in which a large variety of complex organic molecules, some of them typical of hot cores, have been found: CH₃O, CH₃OCOH, CH₃OCH₃, CH₃CHO, and CH₃SH. The abundances of these species relative to H₂, $X \approx 10^{-11}$ (Cernicharo et al. 2012), are much lower in B1-b than in Orion. Using the data from Cernicharo et al. (2012) we have obtained an upper limit for the column density of CH₃NCO in B1-b of $2 \times 10^{11} \text{ cm}^{-2}$ ($X \approx 2 \times 10^{-12}$).

CH₃NCO has also been found towards Sgr B2 by Halfen et al. (2015). They derive a rather low rotational temperature, $T_{\text{rot}} \approx 24 \text{ K}$. However, we have searched for CH₃NCO in other public line surveys of Sgr B2 (Belloche et al. 2013) and found clear identification of methyl isocyanate in the warm gas of Sgr B2, with $T_K \approx 200 \text{ K}$ and $N(\text{CH}_3\text{NCO}) = 5 \times 10^{17} \text{ cm}^{-2}$ for the 63 km s⁻¹ component and $3 \times 10^{17} \text{ cm}^{-2}$ for the second component at 73 km s⁻¹ (see Appendix B). Using our laboratory frequencies, partition function and energy of the levels we have been able to identify 76 lines (43 unblended and 33 partially blended) in the 3 mm Sgr B2(N) data of Belloche et al. (2013). Several lines claimed missing in Halfen et al. (2015) are in fact well detected, but at $\approx 10 \text{ MHz}$ from the predictions they use (see Fig. B. 2). Most of the lines shown in Fig. B.2 have not been detected by Halfen et al. (2015) since they correspond to CH₃NCO transitions with $K \geq 2$ and/or $m \geq 2$. Assuming the column densities derived by Belloche et al. (2013) for the hot component at 200 K and $v_{\text{LSR}} \approx 63 \text{ km s}^{-1}$, we derive $N(\text{CH}_3\text{OH})/N(\text{CH}_3\text{NCO}) \approx 40$, $N(\text{HNCO})/N(\text{CH}_3\text{NCO}) \approx 40$, and $N(\text{CH}_3\text{CN})/N(\text{CH}_3\text{NCO}) \approx 50$, which are different from the values we derived for Orion KL (see Table B.1): 400, 15, 10, and 225, 15, 25, in positions A and B, respectively. The measured difference in the abundance ratio between the two regions again points to a combination of physical and chemical differences based on the evolutionary states of the clouds found in the Galactic centre and outer disk of the Galaxy.

Nothing is known about the formation of methyl isocyanate in the gas phase or on the surface of the grains in molecular clouds. Some gas phase reactions that could form CH₃NCO have been discussed by Halfen et al. (2015). However, the high abundance for this species presently found in Orion and Sgr B2, together with the fact that it is detected in hot cores and not in cold dark clouds, also point towards a chemistry conducted in the grain mantles. Dedicated laboratory experiments on ices have to be performed in order to learn about the formation processes of CH₃NCO. In the ices CH₃NCO could be formed by methylation of HNCO (Goesmann et al. 2015). It is well known that at ambient temperature methyl isocyanate reacts with many substances that contain N–H or O–H groups and with water, which are common in the gas phase of Orion. Hence, the observed differences in molecular abundances between the gas phase and in the comet ice, if the comet surface still keeps pristine dust grains, imply a very rich chemistry in the gas phase for the molecules escaping the ices. Molecular abundances in Orion could result from the chemical history of the ejected material from the grains. It will be of great interest to observe the coma of the comet in order to obtain the abundances of the gas phase species and information on how the COSAC identified molecules survive ejection from the comet surface.

Supplementary Material

Refer to Web version on PubMed Central for supplementary material.

Acknowledgements

The Spanish authors thank MINECO for funding support from the CONSOLIDER-Ingenio program “ASTROMOL” CSD 2009-00038, AYA2012-32032, CTQ 2013-40717 P, CTQ 2010-19008, and the ERC synergy grant ERC-2013-Syg-610256-NANOCOSMOS. They also thank Junta de Castilla y León under grants VA070A08 and VA175U13. Z.K. acknowledges a grant from the Polish National Science Centre, decision number DEC/2011/02/A/ST2/00298. J.-C.G. and J.C. thank the ANR-13-BS05-0008-02 IMOLABS. J.-C.G. thanks the Program PCMI (INSU-CNRS) and the Centre National d’Etudes Spatiales (CNES) for funding support. The OSU authors acknowledge funding from NASA, NSF, and the Army Research Office.

References

- Alonso JL, Lorenzo FJ, López JC, et al. *Chem Phys.* 1997; 218:267.
- Alonso ER, Kolesníková L, Peña I, et al. *J Mol Spectrosc.* 2015; 316:84.
- Becklin EE, Neugebauer G. *ApJ.* 1967; 147:799.
- Bell T, Cernicharo J, Viti S, et al. *A&A.* 2014; 218:72.
- Belloche A, Müller HPS, Menten KM, et al. *A&A.* 2013; 559:A47.
- Bermúdez C, Mata S, Cabezas C, Alonso JL. *Angew Chem Int Ed.* 2014; 53:11015.
- Biver N, et al. *Science Advances.* 2015 in press.
- Blake GA, Sutton EC, Masson CR, Philips TG. *ApJ.* 1987; 315:621.
- Bockelée-Morvan D, Lis DC, Winkler JE, et al. *A&A.* 2000; 353:1101.
- Brändström A, Lamm B, Palmert I. *Acta Chem Scand B.* 1974; 28:699.
- Brouillet N, Despois D, Lu X-H, et al. *A&A.* 2015; 576:A129.
- Brown GG, Dian BC, Douglass KO, et al. *Rev Sci Instrum.* 2008; 79:053103. [PubMed: 18513057]
- Carvajal M, Margulès L, Tercero B, et al. *A&A.* 2009; 500:1109.
- Cernicharo, J. Internal IRAM report. Granada: IRAM; 1985.
- Cernicharo, J. In: Stehl. C.; Joblin, C.; d’Hendecourt, L., editors. *ECLA-2011: Proceedings of the European Conference on Laboratory Astrophysics*, EAS Publications Series; Cambridge: Cambridge Univ. Press; 2012. p. 251
- Cernicharo J, Marcelino N, Roueff E, et al. *ApJ.* 2012; 759:L43.
- Cernicharo J, Tercero B, Fuente A, et al. *ApJ.* 2013; 771:L10.
- Coudert LH, Drouin BJ, Tercero B, et al. *ApJ.* 2013; 779:119.
- Crovisier, J. In: Lazzaro, D.; Ferraz Mello, S.; Fernández, JL., editors. *Asteroids, Comets, Meteors, Proceedings of the 229th Symposium of the IAU*; Cambridge Univ. Press; 2006. p. 133
- Curl RF, Rao VM, Sastry KVLN, Hodgeson JA. *J Chem Phys.* 1963; 39:3335.
- Daly AM, Bermúdez C, López A, et al. *ApJ.* 2013; 768:81.
- Daly AM, Kolesníková L, Mata S, Alonso JL. *J Mol Spectrosc.* 2014; 306:11.
- Daly AM, Bermúdez C, Kolesníková L, Alonso JL. *ApJS.* 2015; 218:30.
- Demyk K, Mäder H, Tercero B, et al. *A&A.* 2007; 466:255.
- Domenech JL, Cueto M, Herrero VJ, et al. *ApJ.* 2013; 771:L11.
- Esplugues GB, Tercero B, Cernicharo J, et al. *A&A.* 2013a; 556:A143.
- Esplugues GB, Cernicharo J, Viti S, et al. *A&A.* 2013b; 559:A51.
- Favre C, Wootten HA, Remijan AJ, et al. *ApJ.* 2011; 739:L12.
- Feng SY, Beuther H, Henning T, et al. *A&A.* 2015; 581:71.
- Fortman SM, McMillan JP, Neese CF, et al. *JMoSp.* 2012; 280:11.
- Friedel DN, Widicus Weaver SL. *ApJS.* 2012; 201:17.
- Genzel R, Stutzki J. *ARAA.* 1989; 27:41.
- Gezari DY, Backman DE, Werner MW. *ApJ.* 1998; 509:283.
- Goesmann F, Rosenbauer H, Hendrik Bredehöft J, et al. *Science.* 2015; 349:aab0689–1. [PubMed: 26228156]
- Goicoechea JR, Chavarría L, Cernicharo J, et al. *ApJ.* 2015; 799:102.

- Gómez L, Rodríguez LF, Loinard L, et al. *ApJ*. 2005; 635:1166.
- Grabow JU, Stahl W, Dreizler H. *Rev Sci Instrum*. 1996; 67:4072.
- Guélin M, Brouillet N, Cernicharo J, Combes F, Wooten A. *Ap&SS*. 2008; 313:45.
- Halfen DT, Ilyushin VV, Ziurys L. *ApJ*. 2015; 812:L5.
- Haykal I, Margulès L, Huet TR, et al. *ApJ*. 2013; 777:120.
- Haykal I, Carvajal M, Tercero B, et al. *A&A*. 2014; 568:58.
- Herbst E, van Dishoeck E. *ARAA*. 2009; 47:427.
- Högbom JA. *A&AS*. 1974; 15:417.
- Kisiel, Z. *Spectroscopy from Space*. Demaison, J., et al., editors. Kluwer Academic Publishers; Dordrecht: 2001. p. 91-106.
- Kisiel, Z. PROSPE Programs for ROtational SPEctroscopy. 2001a. available at www.ifpan.edu.pl/~kisiel/prospe.htm
- Kisiel Z, Pszczółkowski L, Medvedev IR, et al. *J Mol Spectrosc*. 2005; 233:231.
- Kisiel, Z.; Fortman, S.; Medvedev, IR., et al. 65th International Symposium on Molecular Spectroscopy; Columbus, Ohio. June 21-25 (2010); 2010. RC18 https://molspect.chemistry.ohio-state.edu/symposium/_65/symposium/Abstracts/p272.pdf
- Kisiel Z, Pszczółkowski L, Drouin BJ, et al. *J Mol Spectrosc*. 2012; 280:134.
- Kisiel, Z.; Kolesnikova, L.; Alonso, JL., et al. 70th International Symposium on Molecular Spectroscopy; Champaign-Urbana, Illinois. June 22-26 (2015); 2015. TG08 http://isms.illinois.edu/2015/schedule/abstract_files/1046.pdf
- Kleinmann DE, Low FJ. *ApJ*. 1967; 149:L1.
- Kolesniková L, Daly AM, Alonso JL, Tercero B, Cernicharo J. *J Mol Spectrosc*. 2013; 289:13.
- Kolesniková L, Tercero B, Cernicharo J, et al. *ApJ*. 2014; 784:L7.
- Kolesniková L, Peña I, Alonso JL, et al. 2015; 577:A91.
- Koput J. *J Mol Spectrosc*. 1984; 106:12.
- Koput J. *J Mol Spectrosc*. 1986; 115:131.
- Koput J. *J Mol Spectrosc*. 1988; 127:51.
- Kasten W, Dreizler H. *Z Naturforsch*. 1986; 41a:637.
- Lett RG, Flygare WH. *J Chem Phys*. 1967; 47:4730.
- López A, Tercero B, Kisiel Z, et al. *A&A*. 2014; 572:44.
- Marcelino N, Cernicharo J, Tercero B, Roueff E. *ApJ*. 2009; 690:L27.
- Margulès L, Motiyenko RA, Demyk K, et al. *A&A*. 2009; 493:565.
- Margulès L, Huet TR, Demaison J, et al. *ApJ*. 2010; 714:1120.
- Mata S, Peña I, Cabezas C, et al. *J Mol Spectrosc*. 2012; 280:91.
- Medvedev I, Winniewisser M, De Lucia FC, et al. *J Mol Spectrosc*. 2004; 228:314.
- Menten KM, Reid MJ. *ApJ*. 1995; 445:L157.
- Menten KM, Reid MJ, Forbrich J, Brunthaler A. *A&A*. 2007; 474:515.
- Motiyenko RA, Tercero B, Cernicharo J, Margulès L. *A&A*. 2012; 548:A71.
- Mumma MJ, Charnley SB. *ARAA*. 2011; 49:471.
- Muñoz Caro GM, Dartois E. *Chem Soc Rev*. 2013.; 42:2173. [PubMed: 23340705]
- Neill JL, Muckle MT, Zaleski DP, et al. *ApJ*. 2012; 755:153–143.
- Neill J, Crockett NR, Bergin EA, et al. *ApJ*. 2013; 777:85.
- O'Dell CR. *ARAA*. 2001; 39:99.
- Pardo JR, Cernicharo J, Serabyn E. *IEEE Trans Antennas and Propagation*. 2001; 49:12.
- Pascal R, Boiteau L, Commeyras A. *Top Curr Chem*. 2005; 259:69.
- Pasinski T, Westwood NPC. *J Phys Chem A*. 2001; 105:1244.
- Peng T-C, Despois D, Brouillet N, Parise B, Baudry A. *A&A*. 2012; 543:A152.
- Peng T-C, Despois D, Brouillet N, et al. *A&A*. 2013; 554:A78.
- Petkie DT, Goyette TM, Bettens RPA, et al. *Rev Sci Instrum*. 1997; 68:1675.

- Pickett HM. *J Mol Spectrosc.* 1991; 148:371. SPFIT/SPCAT package available at <http://spec.jpl.nasa.gov>.
- Pickett HM, Poynter RL, Cohenet EA, et al. *J Quant Spectrosc & Rad Transfer.* 1998; 60:883.
- Pulliam RL, McGuire BA, Remijan AJ. *ApJ* 751. 2012; 1
- Remijan AJ, Hollis JM, Lovas FJ, Plusquellic DF, Jewell PR. *ApJ.* 2005; 632:333.
- Rodríguez LF, Zapata LA, Ho PTP. *ApJ.* 2009; 692:162.
- Schilke P, Benford DJ, Hunter TR, et al. *ApJS* 132:281–364.
- Shuping RY, Morris M, Bally A. *ApJ.* 2004; 128:363.
- Tercero B, Cernicharo J, Pardo JR, Goicoechea JR. *A&A.* 2010; 517:A96.
- Tercero B, Vincent L, Cernicharo J, Viti S, Marcelino N. *A&A.* 2011; 528:26.
- Tercero B, Margulès L, Carvajal M, et al. *A&A.* 2012; 538:A119.
- Tercero B, Kleiner I, Cernicharo J, et al. *ApJ.* 2013; 770:L13.
- Tercero B, Cernicharo J, López A, et al. *A&A.* 2015; 582:L1.
- Watson, JKG. *Vibrational Spectra and Structure.* Durig, JR., editor. Vol. 6. Elsevier; New York/Amsterdam: 1997. p. 1-89.
- Widicus Weaver SL, Friedel CN. *ApJS.* 2012; 201:16.
- Winnewiser M, Pearson EF, Galica J, Winnewisser BP. *J Mol Spectrosc.* 1982; 91:255.
- Winnewisser BP, Reinstädler J, Yamada KMT, Behrend J. *J Mol Spectrosc.* 1989; 136:12.
- Wynn-Williams CG, Genzel R, Becklin EE, Downes D. *ApJ.* 1984; 281:172.
- Wu Y, Liu T, Qin S-L. *ApJ.* 2014; 791:123.
- Zapata LA, Schmid-Burgk J, Menten KM. *A&A.* 2011; 529:A24.

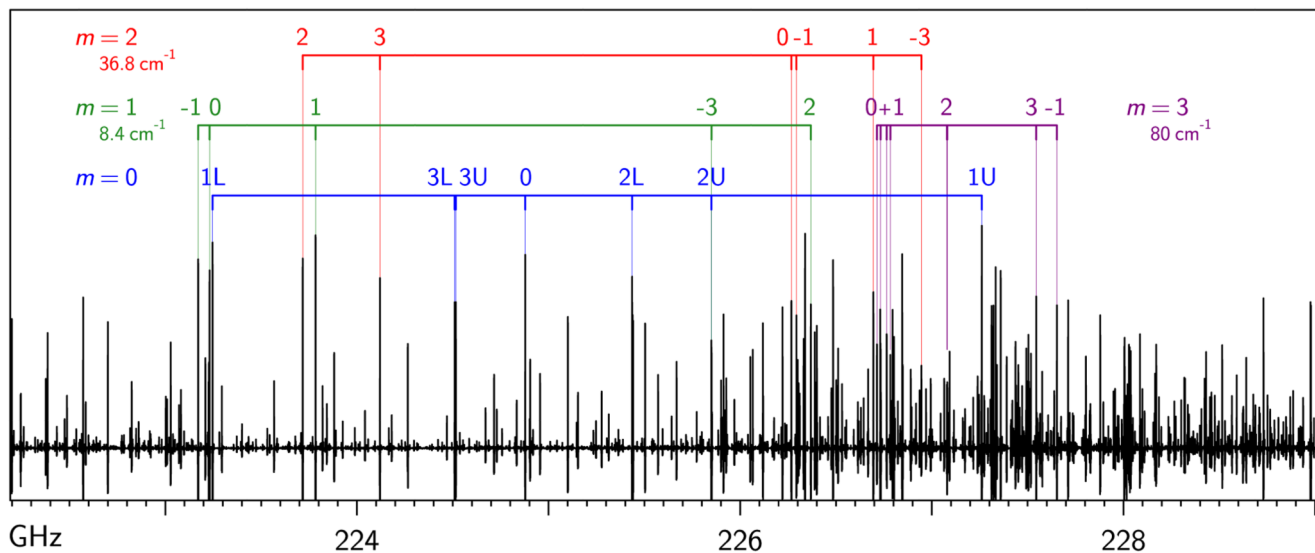


Fig. 1.

Room-temperature rotational spectrum of CH_3NCO in the $J=26-25$ transition region. The spectrum is devoid of features that normally aid assignment, such as identifiable progressions of transitions in rotational or vibrational quantum numbers. The visible complexity is due to the presence of nearly free internal rotation of the methyl group (described by the quantum number m) and the low-frequency CNC bending motion. Vibrational energies of the lowest m states relative to the ground state ($m=0$) and the K assignment are indicated. The high density of states leads to perturbations in frequencies of many transitions, such as the considerable shift to low frequency of the ground state $K=3$ lines.

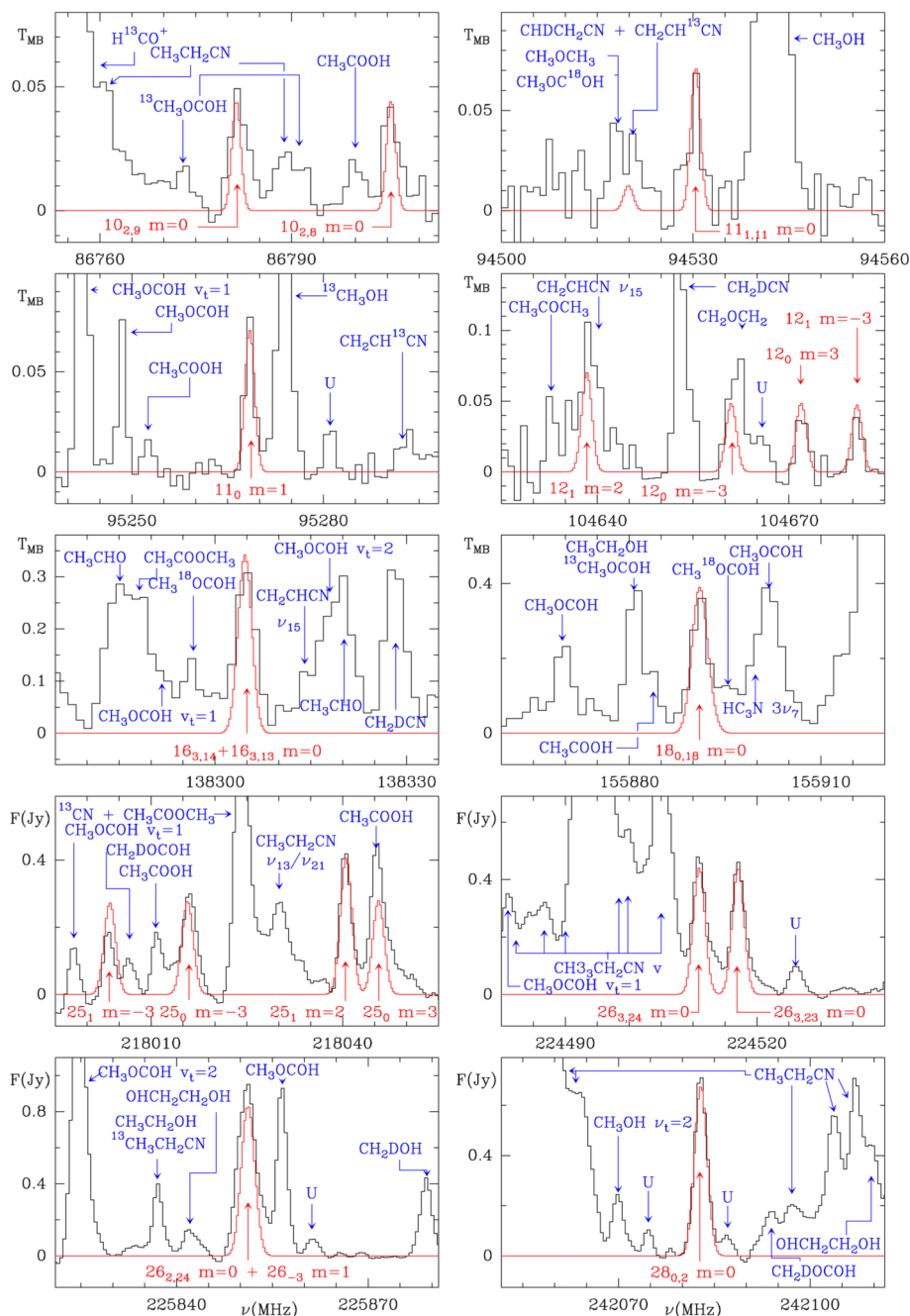
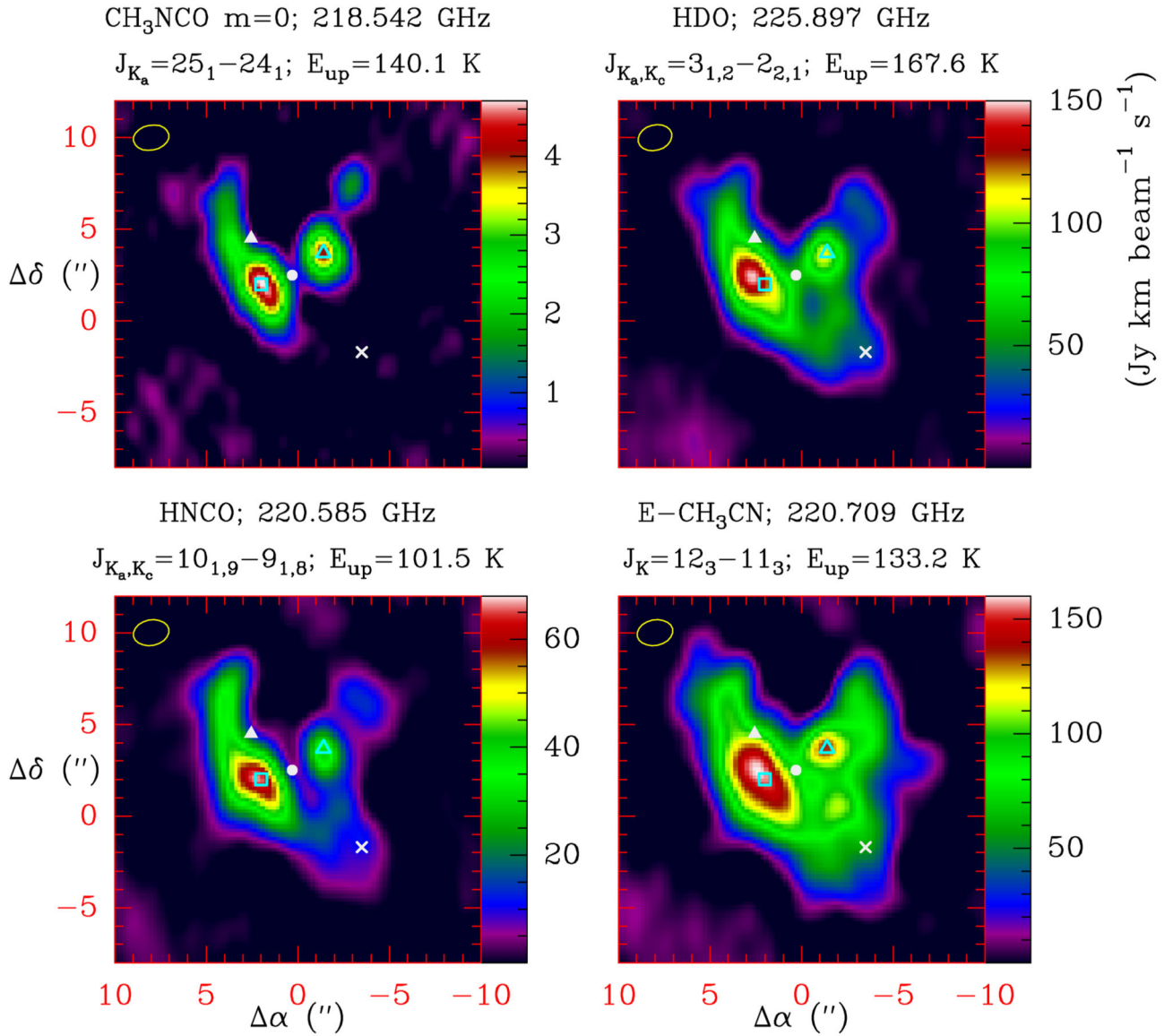


Fig. 2. Selected lines of CH_3NCO as observed with the IRAM 30m radio telescope (toward the IRc2 source at $\alpha_{2000.0} = 5^{\text{h}}35^{\text{m}}14.^{\text{s}}5$, $\delta_{2000.0} = -5^{\circ}22'30''.0$, $0.5''$ north to source *I*, see Fig. 3) and the ALMA interferometer (Position A, see Fig. 3). The red lines show the model of CH_3NCO emission discussed in the text. Red labels show the quantum numbers of the corresponding lines. Blue labels show the species responsible for the other features observed in each panel. The complete set of detected lines of CH_3NCO is shown in Fig. B.1. The intensity units for the last four panels (ALMA data) are in Jy/beam. They can be transformed

into brightness temperature, T_B , by multiplying the intensities by a factor of 9. The intensity scale for the 30m IRAM telescope is the main-beam antenna temperature in K.

**Fig. 3.**

Spatial distribution of CH₃NCO (top left panel) together with those of several molecular species as identified at the top of each panel. The data are from ALMA Science Verification observations. The different positions discussed in the text are indicated by symbols (white triangle: source *I*; white circle: source *n*; ×: the compact ridge; cyan unfilled square/triangle: positions A/B, which are the two emission peaks of CH₃NCO). Additional molecular emission maps are shown in Fig. B.3.